Journal Pre-proof

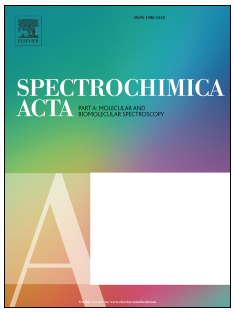

Rapid and label-free metamaterial-based biosensor for fatty acid detection with terahertz time-domain spectroscopy

Mingjie Tang, Liangping Xia, Dongshan Wei, Shihan Yan, Mingkun Zhang, Zhongbo Yang, Huabin Wang, Chunlei Du, Hong-Liang Cui

PII: S1386-1425(19)31126-6

DOI: https://doi.org/10.1016/j.saa.2019.117736

Reference: SAA 117736

To appear in: *Spectrochimica Acta Part A: Molecular and Biomolecular Spectroscopy*

Received Date: 12 August 2019

Revised Date: 22 October 2019

Accepted Date: 30 October 2019

Please cite this article as: M. Tang, L. Xia, D. Wei, S. Yan, M. Zhang, Z. Yang, H. Wang, C. Du, H.-L. Cui, Rapid and label-free metamaterial-based biosensor for fatty acid detection with terahertz time-domain spectroscopy, *Spectrochimica Acta Part A: Molecular and Biomolecular Spectroscopy* (2019), doi: https://doi.org/10.1016/j.saa.2019.117736.

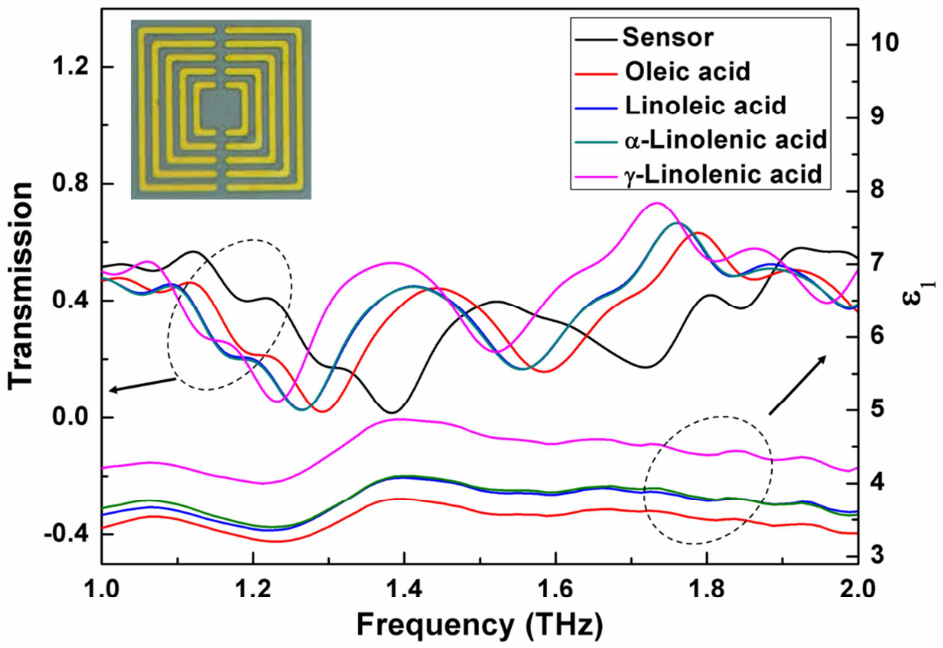

Rapid and label-free metamaterial-based biosensor for fatty acid detection with terahertz time-domain spectroscopy

Mingjie Tang[a,b], Liangping Xia[a,c], Dongshan Wei[a,d], Shihan Yan[a], Mingkun Zhang[a], Zhongbo Yang[a], Huabin Wang[a], Chunlei Du[a*], and Hong-Liang Cui[a*]

[a]Chongqing Key laboratory of Multi-Scale manufacturing Technology, Chongqing Institute of Green and Intelligent Technology, Chinese Academy of Sciences, Chongqing 400714, China
[b]University of Chinese Academy of Science, Beijing 100049, China
[c]School of Electronic Information Engineering, Yangtze Normal University, Chongqing 408100, China
[d]School of Electrical Engineering and Intelligentization, Dongguan University of Technology, Dongguan 523808, Guangdong, China

Abstract: A rapid method for detecting fatty acids (FAs) using terahertz time-domain spectroscopy (THz-TDS) technology combined with a metamaterial-based THz sensor was developed. We measured the THz responses to oleic acid, linoleic acid and α-linoleic acid with different numbers of double-bond, α-linoleic acid and γ-linoleic acid with different conformations. In addition, in order to explore the reason for the observed redshifts of the resonance frequencies of the four FAs, the dielectric constants of the FAs were measured in the THz region. Furthermore, the four fatty acids were also attempted to be identified by Raman spectroscopy, which was difficult to accomplish unambiguously because of the effect of fluorescence. This result thus demonstrates the power and usefulness of metamaterial-assisted THz-TDS in the rapid determination of the FAs, and its potential as a versatile tool for investigation of biological metabolism, and for food product quality, safety inspection and control.

Key words: fatty acid; terahertz time-domain spectroscopy; label-free; THz sensor; dielectric constant

Introduction

Fatty acids (FAs) are widely distributed in nature and are as important as nutritional substances and metabolites in living organisms. FAs play essential roles in biological tissues and as constituents of lipids in biological membranes influence their properties such as fluidity, integrity and the activities of membrane-bound enzymes [1]. Fatty acids are usually analyzed by gas chromatography-mass spectrometry (GC-MS) with derivatization [2] and are routinely identified by comparing retention index (equivalent chain length, ECL [3]) with those of the authentic fatty acid methyl esters (FAME) standards, and/or by executing a similarity search in a reference mass spectra library [4-6].

Many kinds of fatty acids play an important role in trace levels of the regulation of a variety of physiological and biological functions. Most fatty acids show neither natural absorption in the visible and UV regions nor fluorescence, thus their detection at trace levels using absorptiometry is fairly difficult if not impossible [7]. Their biological activities depend greatly on the number, geometry, and arrangement of double bonds [8]. Due to the importance of the location of the double bonds in unsaturated long-chain fatty acids (positional isomers), they have been studied by using fast atom bombardment (FAB) MS–MS , and electrospray ionization (ESI) MS techniques in various fatty acids [9].

In recent years, THz spectroscopy has emerged as a promising technique that enables label-free, noncontact, and non-destructive inspection of chemical and biological substances [10-19]. THz detection of FAs has shown a great deal of advantages while avoiding the usual significant loss of THz wave transmission in other biological matters imbued with water. Several sharp peaks were observed for saturated crystallized fatty acids [20, 21], and unsaturated crystallized fatty acids showed two distinct peaks (at 247 and 328 cm^{-1}), signifying that the carboxylic group THz absorbance of fatty acids was concentration-dependent [22]. However, for non-crystallized materials, their terahertz absorption spectra are often featureless which makes it hard to identify a material with good specificity.

Metamaterials consist of periodically arranged, sub-wavelength metallic and/or dielectric elements and are designed to exhibit unique electromagnetic properties such as negative refraction [23, 24], sub-diffraction limited focusing [25-27], and cloaking [28, 29]. In addition, metamaterials with gap structures are endowed with strongly localized and enhanced fields, enabling sensitive detection of minute amounts of chemical and biological substances [30-36]. A well-designed metamaterial sensor would be so extraordinarily sensitive to the substance deposited over its surface, that it could provide a feasible approach to detect fatty acids with an extremely thin layer. Similar metamaterial sensors have been used to quantitatively analyze dilute BSA solution [37] and to track the loss of extracellular and intracellular water [38].

In this work, we performed THz TDS on THz metamaterial sensors for high-speed detection of FAs of different double-bond numbers (Oleic acid, linoleic acid, α-linoleic acid) and positional isomers (α-linoleic acid, γ-linoleic acid). We measured frequency shifts in the inductive-capacitive resonance following the deposition of FAs (Oleic acid, linoleic acid, α-linoleic acid, γ-linoleic acid) with very low surface density. The resonance frequency shift in the specifically designed THz metamaterial was studied as a function of the effective dielectric constant, which was found to be consistent and in quantitative correlation with the dielectric constant measurements of individual FAs. In addition, the four kinds of fatty acids were detected by Raman spectroscopy. It was found that the Raman signal of linolenic acid could not be obtained simply because of the influence of fluorescence.

Materials and methods

Sample preparation

The THz sensor composed of metallic square arrays of five square rings with two micro-gaps in the ring was fabricated by the conventional photo-lithography technique on a high resistance silicon (Si) substrate with the thickness of 400 μm. 20 nm thick Chromium (Cr) and 200 nm thick gold (Au) metal films were successively deposited on the Si substrate in order to pattern the split-ring

resonator (SRR) structure with a period of 60 μm, gap size of 2.5 μm, linewidth of 2 μm, and line-length of 50 μm, as depicted in Fig. 1.

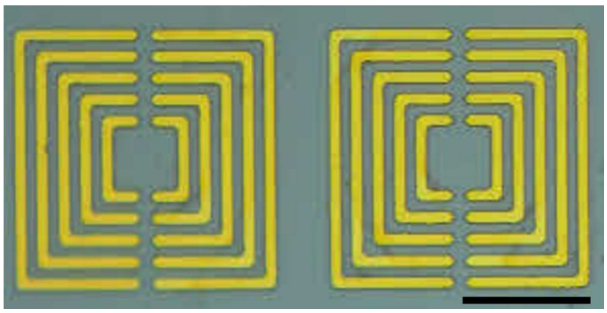

Fig.1 Structural schematic of the metamaterial sensor. The figure shows two adjacent elements of the 150 by 150 array of concentric gapped square rings on the sensor chip. Scale bar: 25 μm.

Oleic acid, linoleic acid, α-linoleic acid and γ-linoleic acid were purchased from Sigma, with schematic diagram of chemical structures shown in Fig. 2. The sample (1 μL) was dropped on the cleaned surface of the THz sensor, and then coated evenly on the surface with the sample using a spin coater prior to experiments. After THz-TDS measurement of one sample, The THz sensor coated with the FAs was washed by ethanol and ultra-pure water and then dried by nitrogen before switching to other samples. The same thickness of the samples was ensured by the same amount of samples deposited on the sensor surface.

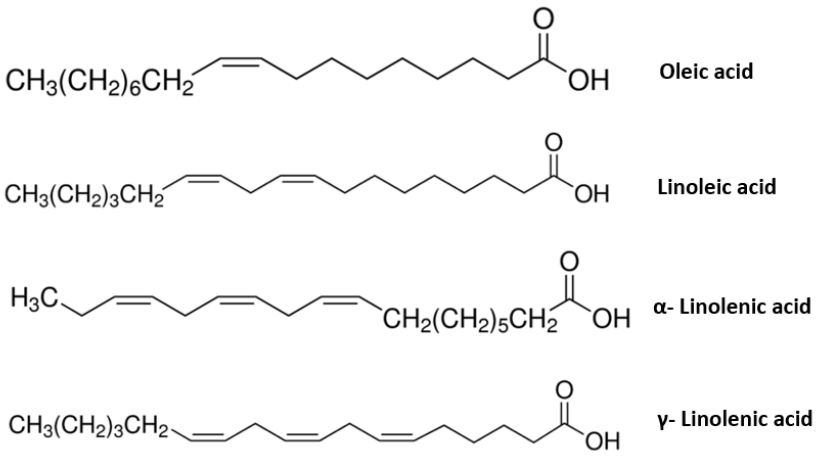

Fig. 2 Chemical structures of the tested FAs.

THz spectroscopy measurement

THz transmission spectra were measured by employing a commercial THz-TDS system (Advanced Photonix, Inc., T-Ray 5000). The femtosecond pulses were produced by a Ti-sapphire laser with a

central wavelength of 1064 nm, a repetition rate of 100 MHz, and pulse duration of <100 fs; The beam was divided into two parts by a polarizing beam splitter, one as the probe beam, directly irradiating on the photoconductive antenna (PCA), another as the pump light gathering on another PCA that had been biased electrically to generate THz radiation, with an average power of 130 nW, which was focused on and penetrated the metamaterial. The THz signals irradiated on the second PCA were sampled discretely by the probe light to acquire the time-domain waveforms.

THz time-domain waveforms of the THz sensor covered with FAs were acquired under the same experimental conditions, at room temperature of 25℃ and a relative humidity of 3%, maintained by the purge of nitrogen gas. Triplicates were run per sample. An average THz time-domain waveforms of each fatty acid was obtained in the 1.0 to 2.0 THz band.

First, the dielectric constants of four fatty acids were measured by terahertz transmission spectroscopy to aid the verification of the relationship between the dielectric constants and THz time-domain waveforms detected by terahertz combined with metamaterial sensor. Each sample solution (about 7 μL) is respectively injected into a liquid sample cells, which has a diameter of 9 mm, thickness of 0.12 mm, featuring two plastic (Polyvinyl Chloride) slide windows sandwiching a Secure-Seal spacer. The cells are prepared for the four FAs (Oleic acid, linoleic acid, α-linoleic acid, γ-linoleic acid). The same sample cell with fixed thickness and diameter is used for each sample and is disposable after use. THz transmission spectra of the FAs in the sample cells were collected. Triplicates were run per sample. An average dielectric constant of each fatty acid was calculated in the THz region.

The THz optical refractive index of the FAs is calculated using a standard approach [39],

(1) $\mathrm{n}(\omega) = \frac{|\varphi_s(\omega) - \varphi_{ref}(\omega)|.c}{\omega d} + 1,$

where $\varphi_s(\omega), \varphi_{ref}(\omega)$ are the phase angles of the Fourier transforms of the power transmissions of the FA sample I_s, and the power transmissions of the reference (the blank sample cell), I_{ref}, respectively, and c is the light speed and ω is the angular frequency. To derive the

dielectric constant, the extinction coefficient, $\kappa(\omega)$, was obtained first, as,

(2) $\kappa(\omega) = ln\left[\frac{4n(\omega)}{\rho(\omega)[n(\omega)+1]^2}\right]\frac{c}{\omega d}$,

where $\rho(\omega)$ is the amplitude ratio of the Fourier transforms of I_s and I_{ref}. The absorption coefficient of the FAs, α, is deducted as

(3) $\alpha(\omega) = 2\omega\kappa(\omega)/c$,

and the complex dielectric constant, $\hat{\varepsilon}(\omega)$, is expressed as

(4) $\hat{\varepsilon}(\omega) = [n(\omega) + i\kappa(\omega)]^2 = \varepsilon_1 + i\varepsilon_2$,

where ε_1 and ε_2 are the real part and the imaginary part of the dielectric constant, respectively.

Raman spectroscopy measurement

Raman spectra were measured by employing a Renishaw inVia Raman spectrometer which was made in UK. In order to reduce the background of the Raman spectra, the 10 μL FAs were dripped on the surface of MgF_2. In this experiment, the wavelength of the excitation laser is 532 nm. The system was calibrated with a small piece of clean silicon whose peak is located at 520.5 cm^{-1} before measuring the Raman spectra. Three different locations on each FAs were measured to obtain an average spectrum for each sample under the same experimental conditions. The temperature was 25℃ and the humidity was 52% in the laboratory. The effective frequency region ranged from 100 to 3200 cm^{-1}.

Results and discussion

THz detection of FAs

The average THz transmission spectra for the THz sensor covered with four FAs are shown in Fig. 3. A series of resonant frequencies have been observed, and the THz transmission spectrum of the blank dry THz sensor was obtained as a reference, with the resonant frequency of 1.3875 THz. Obviously, compared with the blank THz sensor, the resonant frequencies of the samples were redshifted. The amounts of shifts for three representative resonant frequencies were 87.5 GHz, 112.5 GHz and 143.75 GHz, respectively. It is a commonly accepted practice to model the

fundamental mode of the SRR as that of an LC oscillator, with a resonant frequency given by $\Omega = 1/\sqrt{LC}$, where L and C are the equivalent inductance and capacitance of the SRR. Consequently the redshift can be explained by the change of capacitance in the gap area, which is proportional to the effective dielectric constant. Apparently, the FAs attached to the THz sensor cause the effective dielectric constant to increase, resulting in the redshift of the resonant frequency.

Standard SPR theory predicts a one-to-one correspondence between the resonant frequency and the effective dielectric constant, based on which we can conclude that there exists three different dielectric constants, corresponding to the three measured resonant frequencies. Oleic acid is an eighteen carbon fatty acid with one double-bond, linoleic acid with two double-bonds, α-linoleic acid and γ-linoleic acid are positional isomers with three double-bonds. Thus the observed different resonant frequencies might be used to characterize the number, geometry and arrangement of double bonds in the THz range.

To further explore the reason for the three kinds of redshifts, we measured the dielectric constants of the FAs in the THz region, as shown in Fig.4. These results revealed that there were also several different values of the dielectric constants, of which we mainly focus on three real part of the dielectric function here. We find that the real part of the dielectric constants showed an increase with increase in the redshifts of resonant frequencies in the THz range. Moreover, as noted before, Oleic acid is fatty acid with one double-bond, linoleic acid with two double-bond, γ-linoleic acid with three double-bond, thus the number of double-bond differentiates the real part of the dielectric constant of these three fatty acids.

At the same time, we found that in the case of linoleic acid (with two double-bond) and α-linoleic acid (with three double-bond), their resonant frequencies were nearly indistinguishable. Thus, the experimental results suggested that there should be similar dielectric constants between linoleic acid and α-linoleic acid. And dielectric constant measurement has suggested that the real part of the dielectric function of linoleic acid and α-linoleic acid were indeed similar. Thus, we could not jump

to a conclusion that dielectric constants showed a linear or nonlinear increase with increase in the number of double-bond in the THz range.

Additionally, it manifested that the dielectric constant of γ-linoleic acid was greater than α-linoleic acid, based on the results that the resonant frequency of γ-linoleic acid (1.24375 THz) was lower than that of α-linoleic acid (1.275 THz) and the formulas mentioned above. It demonstrated that the real part of the complex dielectric constant of FAs was related to the conformation of the molecule. Thus, we could draw a conclusion that when the resonant peak is found at a specific frequency, it indicates that the corresponding dielectric constant would correlate with the conformation of the sample.

To our knowledge there have been no reports on the differences of complex dielectric constants among the four FAs in the THz region. Due to the complex dielectric constants of the FAs influenced by the number, geometry and arrangement (conformation) of double bonds, resonant frequencies among the FAs were obviously different. Thus THz-TDS combined with metamaterial technology could sense the number, geometry and arrangement of double bonds, further distinguishing the FAs. Meanwhile, as is commonly known, there are many kinds of fatty acids in edible oils and in the body of animals and plants, which can be distinguished by the THz-TDS system through improved detection sensitivity by perfecting the design, fabrication, and functional modifications of the metamaterials.

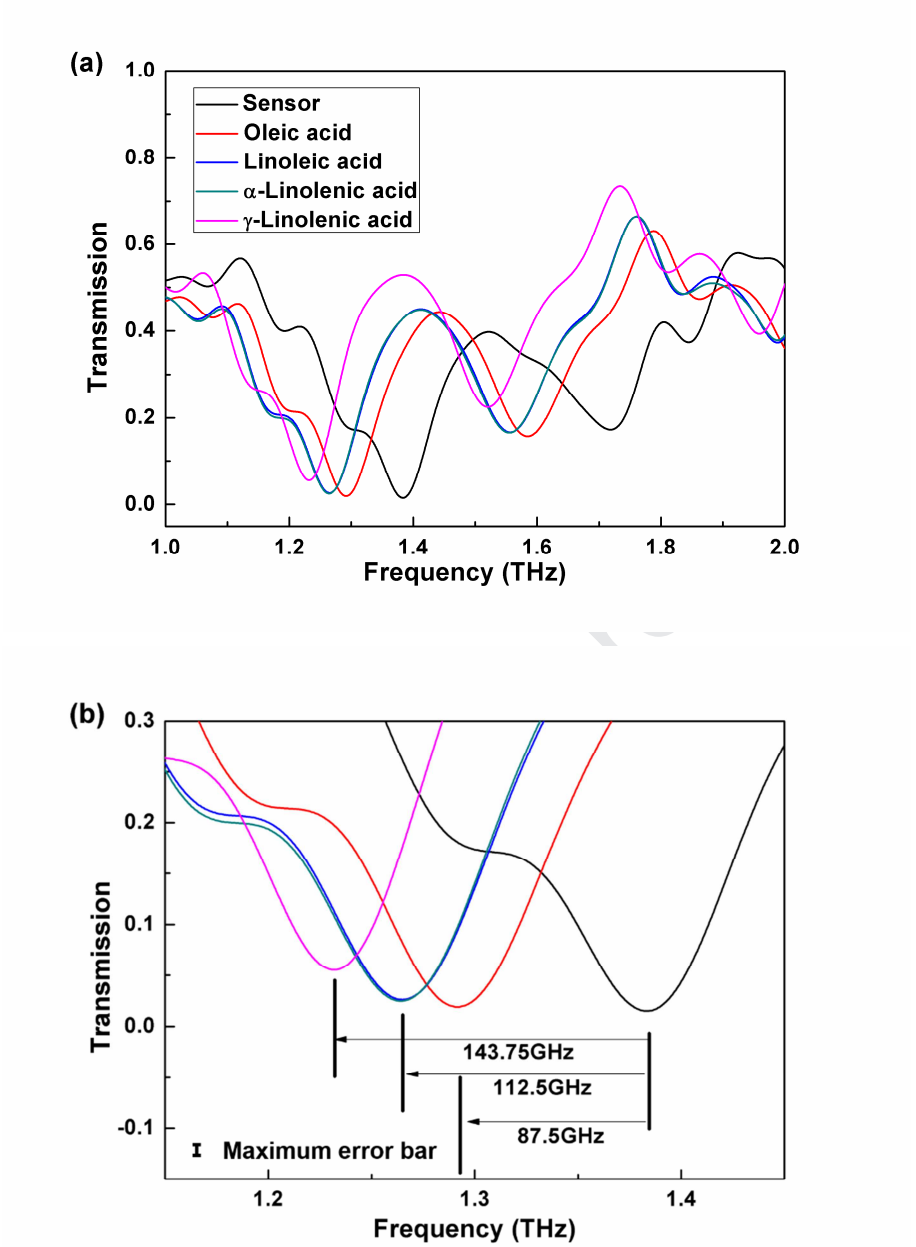

Fig. 3 (a) THz transmission spectra measured with THz sensor coated with the four FAs. (b) is a partially enlarged view of (a).

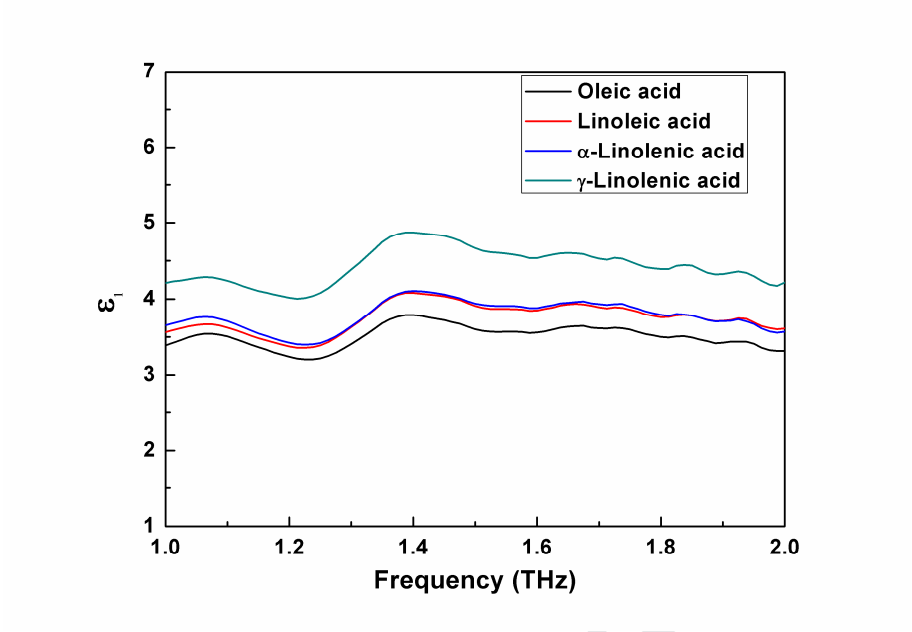

Fig. 4 Real part of the dielectric constants of the FAs in the THz region.

Finite element method simulation

Based on the structural parameters of the metamaterial mentioned in the above part, the surface electromagnetic field distribution of the metamaterial was simulated with the finite element method (FEM). Additionally, the shifts of the resonance frequencies had also been calculated when the dielectric constant of the model was varied from 1.0 to 6.0. The FEM simulation was carried out using a commercial software (COMSOL).

FEM simulation was carried out to predict the surface electromagnetic field distribution of the metamaterial at the 1.3875 THz resonance frequency (Fig. 5). As can be seen, the surface electromagnetic field distribution of the metamaterial is concentrated in the outermost ring. Therefore, the 1.3875 THz resonance was mainly caused by the resonance of the outermost ring.

In order to predict the resonant peak changes, the shifted resonance frequencies had been calculated (Fig. 6). The result showed that there was a good linear correlation between the dielectric constant and the resonance frequency shifts. In addition, the shift of resonance frequency could reach 20 GHz when the dielectric constant increased by 0.5, which was similar with the shift of resonance

frequency observed in the experiment.

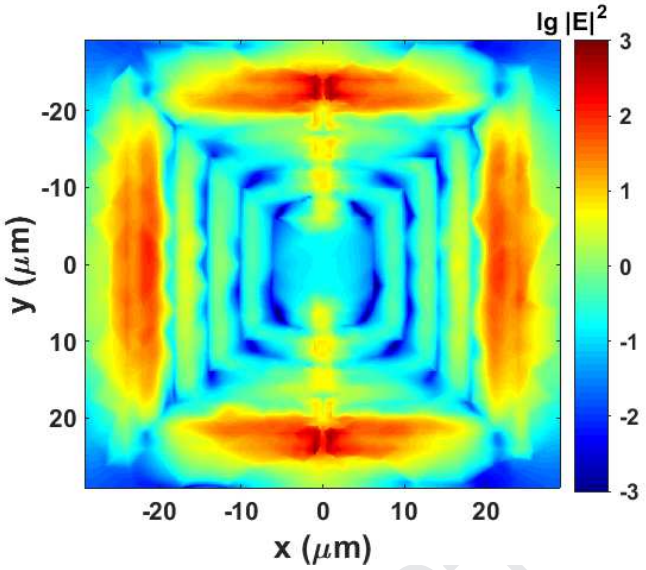

Fig. 5 Simulated surface electromagnetic field distribution of the metamaterial at the 1.3875 THz resonance frequency.

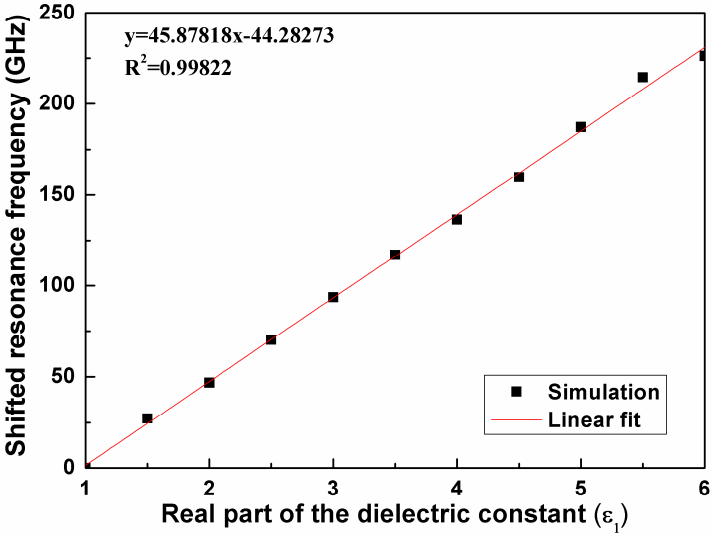

Fig. 6 Correlation between the real part of the dielectric constant and the shifted resonance frequency at the 1.3875 THz resonance.

Raman detection of FAs

Raman spectra of oleic acid and linoleic acid after baseline calibration are shown in Fig. 7. Because the fluorescence intensity produced by α-linoleic acid and γ-linoleic acid is far greater than that of the Raman scattering light, the characteristics of Raman signal are concealed. The Raman characteristic peaks of oleic acid and linoleic acid are basically similar. So it can be concluded that it is difficult to directly distinguish the four fatty acids by Raman spectroscopy.

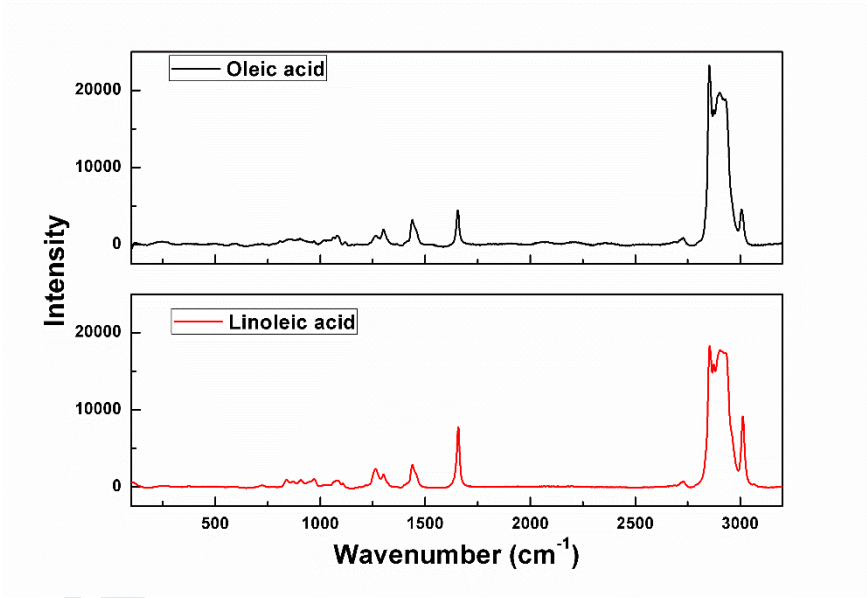

Fig. 7 Raman spectra of oleic acid and linoleic acid.

Conclusion

In conclusion, we have studied the dielectric frequency responses of oleic acid, linoleic acid, α-linoleic acid, and γ-linoleic acid, employing a combination of THz-TDS with a SRR metamaterial-based chip, and observed clear shifts in the resonant frequencies of the samples, attributable to the different double-bond number and conformation of the FAs, due to inherent changes in the dielectric constants in the gap areas of the SRR. Thus, the THz SRR sensor chip provides a potentially powerful approach to distinguish different FAs, because of the strong sensitivity to the samples adhered to the surface of the chip. However, within experimental

resolution there was no discernible difference in the resonant frequencies of linoleic acid and α-linoleic acid. Although the two are similar in molecular structure, there was no apparent reason for them to respond exactly the same way to THz radiation. We suspect that the difference, if there is any, is small, and below our current system resolution. Further improvement in THz technology and THz sensor sensitivity is obviously desirable, by perfecting the design, fabrication and functional modification, which could improve the sensitivity of THz detection to eventually distinguish all the different kinds of FAs, thus finally achieve label-free detection of FAs. In follow-up studies, we will also attempt to use a variety of spectral methods to identify fatty acids with different saturation and conformation.

Acknowledgement

This work was financially supported by the National Key Research and Development Program of China (2017YFF0106303), the Central Government Supported Key Instrument Program of China (YXGYQ201700136), the National Natural Science Foundation of China (61605207, 11604332, 61775213, 61875196), and the Natural Science Foundation of Chongqing (cstc2019jcyj-msxmX0654, cstc2019jcyj-msxmX0352).

References

1. Jalali-Heravi, M. and M. Vosough, *Characterization and determination of fatty acids in fish oil using gas chromatography-mass spectrometry coupled with chemometric resolution techniques.* Journal of Chromatography A, 2004. **1024**(1-2): p. 165-176.

2. Drozd, J., *Chemical Derivatization in Gas-Chromatography.* Journal of Chromatography, 1975. **113**(3): p. 303-356.

3. Miwa, T.K., et al., *Gas Chromatographic Characterization of Fatty Acids - Identification Constants for Monocarboxylic and Dicarboxylic Methyl Esters.* Analytical Chemistry, 1960. **32**(13): p. 1739-1742.

4. Hartig, C., *Rapid identification of fatty acid methyl esters using a multidimensional gas chromatography-mass spectrometry database.* Journal of Chromatography A, 2008. **1177**(1): p. 159-169.

5. Wasta, Z. and S.A. Mjos, *A database of chromatographic properties and mass spectra of fatty acid methyl esters from omega-3 products.* Journal of Chromatography A, 2013. **1299**: p. 94-102.

6. Zhang, L.X., et al., *Establishment of reliable mass spectra and retention indices library: Identification of fatty acids in human plasma without authentic standards.* Talanta, 2012. **88**: p. 311-317.

7. Ingalls, S.T., et al., *Derivatization of Carboxylic-Acids by Reaction with 4'-Bromophenacyl Trifluoromethanesulfonate Prior to Determination by High-Performance Liquid-Chromatography.* Journal of Chromatography, 1984. **299**(2): p. 365-376.

8. Vrkoslav, V. and J. Cvacka, *Identification of the double-bond position in fatty acid methyl esters by liquid chromatography/atmospheric pressure chemical ionisation mass spectrometry.* Journal of Chromatography A, 2012. **1259**: p. 244-250.

9. Hsu, F.F. and J. Turk, *Distinction among isomeric unsaturated fatty acids as lithiated adducts by electrospray ionization mass spectrometry using low energy collisionally activated dissociation on a triple stage quadrupole instrument.* Journal of the American Society for Mass Spectrometry, 1999. **10**(7): p. 600-612.

10. Ferguson, B. and X.C. Zhang, *Materials for terahertz science and technology.* Nature Materials, 2002. **1**(1): p. 26-33.

11. Menikh, A., et al., *Terahertz biosensing technology: Frontiers and progress.* Chemphyschem, 2002. **3**(8): p. 655-658.

12. Markelz, A.G., A. Roitberg, and E.J. Heilweil, *Pulsed terahertz spectroscopy of DNA, bovine serum albumin and collagen between 0.1 and 2.0 THz.* Chemical Physics Letters, 2000. **320**(1-2): p. 42-48.

13. Mickan, S.P., et al., *Label-free bioaffinity detection using terahertz technology.* Physics in Medicine and Biology, 2002. **47**(21): p. 3789-3795.

14. Nagel, M., et al., *A functionalized THz sensor for marker-free DNA analysis.* Physics in Medicine and Biology, 2003. **48**(22): p. 3625-3636.

15. Woodward, R.M., et al., *Terahertz pulsed imaging of skin cancer in the time and frequency domain.* Journal of Biological Physics, 2003. **29**(2-3): p. 257-261.

16. Menikh, A., et al., *Label-free amplified bioaffinity detection using terahertz wave technology.* Biosensors & Bioelectronics, 2004. **20**(3): p. 658-662.

17. George, P.A., et al., *Microfluidic devices for terahertz spectroscopy of biomolecules.* Optics Express, 2008. **16**(3): p. 1577-1582.

18. Alexandrov, B.S., et al., *DNA breathing dynamics in the presence of a terahertz field.* Physics Letters A, 2010. **374**(10): p. 1214-1217.

19. Park, H.R., et al., *Colossal Absorption of Molecules Inside Single Terahertz Nanoantennas.* Nano Letters, 2013. **13**(4): p. 1782-1786.

20. Tanno, T., et al., *Analytical method for studying terahertz vibrations in a stearic acid single crystal.* Infrared Physics & Technology, 2014. **67**: p. 427-431.

21. Fan, S.T., et al., *Correlation between saturated fatty acid chain-length and intermolecular forces determined with terahertz spectroscopy.* Chemical Communications, 2019. **55**(25): p. 3670-3673.

22. Jiang, F.L., et al., *Terahertz Absorption Spectra of Fatty Acids and Their Analogues.* Journal of Oleo Science, 2011. **60**(7): p. 339-343.

23. Pendry, J.B., et al., *Magnetism from conductors and enhanced nonlinear phenomena.* Ieee Transactions on Microwave Theory and Techniques, 1999. **47**(11): p. 2075-2084.

24. Shelby, R.A., D.R. Smith, and S. Schultz, *Experimental verification of a negative index of refraction.* Science, 2001. **292**(5514): p. 77-79.

25. Liu, Z.W., et al., *Far-field optical hyperlens magnifying sub-diffraction-limited objects.* Science, 2007. **315**(5819): p. 1686-1686.

26. Pendry, J.B., *Negative refraction makes a perfect lens.* Physical Review Letters, 2000. **85**(18): p. 3966-3969.

27. Smolyaninov, I.I., Y.J. Hung, and C.C. Davis, *Magnifying superlens in the visible frequency range.* Science, 2007. **315**(5819): p. 1699-1701.

28. Pendry, J.B., D. Schurig, and D.R. Smith, *Controlling electromagnetic fields.* Science, 2006. **312**(5781): p. 1780-1782.

29. Schurig, D., et al., *Metamaterial electromagnetic cloak at microwave frequencies.* Science, 2006. **314**(5801): p. 977-980.

30. Hong, J.T., et al., *Dielectric Constant Engineering of Single-Walled Carbon Nanotube Films for Metamaterials and Plasmonic Devices.* Journal of Physical Chemistry Letters, 2013. **4**(22): p. 3950-3957.

31. Chen, T., S.Y. Li, and H. Sun, *Metamaterials Application in Sensing.* Sensors, 2012. **12**(3): p. 2742-2765.

32. Chang, Y.T., et al., *A multi-functional plasmonic biosensor.* Optics Express, 2010. **18**(9): p. 9561-9569.

33. Park, D.J., et al., *Terahertz near-field enhancement in narrow rectangular apertures on metal film.* Optics Express, 2009. **17**(15): p. 12493-12501.

34. Seo, M.A., et al., *Terahertz field enhancement by a metallic nano slit operating beyond the skin-depth limit.* Nature Photonics, 2009. **3**(3): p. 152-156.

35. Berrier, A., et al., *Detection of deep-subwavelength dielectric layers at terahertz frequencies using semiconductor plasmonic resonators.* Optics Express, 2012. **20**(5): p. 5052-5060.

36. Yen, T.J., et al., *Terahertz magnetic response from artificial materials.* Science, 2004. **303**(5663): p. 1494-1496.

37. Wang, S.J., et al., *Terahertz Biosensing Based on a Polarization-Insensitive Metamaterial.* Ieee Photonics Technology Letters, 2016. **28**(9): p. 986-989.

38. Liu, Y., et al., *Cell viability and hydration assay based on metamaterial-enhanced terahertz spectroscopy.* Rsc Advances, 2017. **7**(85): p. 53963-53969.

39. Kindt, J.T. and C.A. Schmuttenmaer, *Far-Infrared Dielectric Properties of Polar Liquids Probed by Femtosecond Terahertz Pulse Spectroscopy †*. J. Phys. Chem., 1996. **100**(24): p. 10373-10379.

Highlights

- Application of THz TDS on metamaterial biosensors to detect the FAs of different double-bond numbers and positional isomers
- Dielectric constants were measured to aid the verification of the relationship the dielectric constants of the FAs and the offset of the resonant peaks
- The FAs were attempted to be identified by Raman spectroscopy, which was difficult to accomplish unambiguously because of the effect of fluorescence

Declaration of Interest Statement

There are no conflicts to declare.